Cascaded second-order effects in *N*-(4-nitrophenyl)-L-prolinol, in a molecular single crystal

Zuo Wang, David J. Hagan, and Eric W. VanStryland

Center for Research and Education in Optics and Lasers, University of Central Florida, Orlando, Florida 32826

Joseph Zyss and Petar Vidakovik

Centre National des Etudes Telecommunications, 196 Avenue Henri Ravera, 92220 Bagneux, France

William E. Torruellas

Department of Physics, Washington State University, Pullman, Washington 99164

Received January 5, 1996; revised manuscript received May 15, 1996

An investigation of cascaded second-order optical effects resulting in effective third-order interactions, temporal and spatial self-action, are presented for *N*-(4-nitrophenyl)-L-prolinol (NPP) a molecular single crystal with one of the largest phase-matchable second-order nonlinear coefficients known in the visible and near-infrared portions of the spectrum. We emphasize the effects of temporal and spatial walk-off in the nonlinear-optical propagation in NPP and discuss their consequences for cascaded second-order nonlinear applications. Walk-off effects play a detrimental role in cascaded all-optical switching. Whereas in standard second-harmonic generation walk-off reduces the efficiency but does not prevent the generation, in the case of cascading back-conversation is required and more-deleterious effects occur: a portion of the field is lost in that the overlap between fundamental and second-harmonic wavelengths is reduced. © 1997 Optical Society of America. [S0740-3224(97)00101-X]

1. INTRODUCTION

Only a few existing materials have been found to fulfill the nonlinearity–transparency trade-offs for ultrafast nonlinear all-optical switching in the relevant telecommunication windows at multiGbits/s rates.[1] Indeed, it has been shown that when they are far away from the linear absorption edge, materials with large third-order nonlinear-optical coefficients exhibit multiphoton absorption, which in a Kramers–Kronig sense enhances the intensity-dependent refractive nonlinearity.[2] The inability to find advanced highly nonlinear materials with a high enough optical quality to process low-loss waveguide structures has led to a radical new approach to the nonlinear-optical switching problem, cascaded second-order parametric processes.[3]

Early in the investigation of nonlinear-optical effects, Ostrovsky recognized that a material with a phase-matchable second-order process could exhibit effects resembling those expected from a third-order optical response, namely, self-focusing or self-defocusing and temporal self-phase modulation.[4] Such an approach had to wait for the advent during the past few years of commercially available transparent second-order materials, such as potassium titanyl phosphate (KTP), lithium triborate, and β-barium borate, ($d_{\text{eff}} = 1$–3 pm/V) with moderate phase-matchable nonlinearities with exceptionally large optical damage thresholds, in excess of 100 GW/cm^2 for picosecond and femtosecond pulses. Similarly, low-loss waveguides are now designed in technologically advanced materials such as lithium niobate and KTP in most cases with quasi-phase-matched (QPM) gratings. Quasi-phase matching adds the flexibility of engineering the phase-matching resonances, for instance, for telecommunication-oriented applications such as multi-wavelength generation and detection–amplification, and eliminates the spatial walk-off that is due to natural birefringence.[5] This advance in materials and device engineering has rapidly led to the demonstration of device concepts such as nonlinear Mach–Zehnder interferometers in a hybrid or integrated waveguide form, nonlinear directional couplers, and spatial solitons in planar waveguides as well as all-optical switching and solitary waves in bulk materials, all using cascaded second-order nonlinearities.[6–12] Note that new effects, not achievable with a simple cubic optical response, can be observed with this approach. Transistor action and stable multidimensional solitary waves are just two examples of such effects.

The effective third-order refractive nonlinearity imposed on the propagation of a fundamental plane wave or waveguide mode as it propagates in a phase-matched, quasi-resonant, second-order structure is represented by the following expression of the intensity-dependent refractive index[13]:

$$n_2^{\text{eff}} = \frac{2\Omega d_{\text{eff}}^2}{c^2 \epsilon_0 n_1^2 n_2} \frac{[1 - \sin c(\Delta k L)]}{\Delta k L} L, \qquad (1)$$

0740-3224/97/010076-11$10.00

where $n(I) = n_0 + n_2 I$, Ω is the optical angular frequency, d_{eff} is the effective second-order coefficient, $n_{1,2}$ are the refractive indices at the fundamental and second-harmonic frequencies, respectively, and the wave-vector mismatch is represented by $\Delta kL = (k_2 - 2k_1)L$. It is worth noting that the above nonlinear refractive index is length dependent; in other words, it differs from the constant cubic intensity-dependent refractive index that arises from the third-order susceptibility that is responsible for self-action in all materials. Hence n_2^{eff} is sometimes referred to as being nonlocal. Equation (1) should be considered valid for low pump or fundamental depletion (less than 25%) in a material without a center of symmetry and a phase-matchable nonlinear coefficient represented by d_{eff}. In addition, under close phase-matching conditions and large depletions, the fundamental phase distortion does not follow the intensity but instead follows the fundamental field amplitude, as expected in the depleted fundamental regime.[3] We should emphasize at this point that to derive Eq. (1) we assumed no dispersion, all spatial transverse phenomena were neglected, and we dealt with long-pulse or cw operation. From the materials point of view the important material figure of merit $d_{\text{eff}}^2/n_1^2 n_2$ is the same one used for second-harmonic generation.

Organic materials, which have large figures of merit relative to other phase-matchable second-order nonlinear-optical structures, should be well suited for cascaded all-optical applications.[14] In what follows we investigate one such material, *N*-(4-nitrophenyl)-L-prolinol (NPP). Indeed, NPP is known to possess one of the largest phase-matchable d_{eff} known, 85 pm/V at 1064 nm, with refractive indices of 1.7–2, resulting in an excellent figure of merit for both second-harmonic generation (SHG) and cascaded nonlinear-optical effects. Such large nonlinearity is due, at a molecular level, to an optimized charge-transfer exciton, resulting in a broad absorption band that peaks near 370 nm. NPP is thus a yellowish molecular crystal. At a crystalline level the molecules are aligned with an almost ideal orientation for type I interaction, and the refractive-index dispersion results in a wide variety of phase-matching geometries, in particular for parametric downconversion devices.[15–17] Because of the presence of the charge-transfer excitonic band, a strong refractive-index dispersion is observed over the visible and near-infrared portions of the spectrum. As a consequence, relatively narrow phase-matching resonances are obtained. More importantly, as discussed here, large temporal and spatial walk-off effects are observed, limiting the efficiency of NPP for cascading applications. Here we discuss the regime in which Eq. (1) fails to predict and to scale properly the nonlinear cascaded effects and for which a more accurate wave propagation analysis needs to be introduced, in particular to deal with walk-off effects.

In what follows we introduce the effects of walk-off in the temporal regime, using a model that is independent of the transverse spatial dimension. Such an approach can be immediately translated into a transverse propagation problem in space, for instance, in a planar waveguide. We follow this introduction to the walk-off problem with a similar approach in which we look at the effects of spatial walk-off for a two-dimensional transverse beam focused upon a NPP single crystal and compare them with our experimental results at 1064 nm with relatively long pulses of 30 ps (FWHM). Finally, to model our experiments in a spectral region where spatial walk-off can be neglected, we introduce a time–space propagation model that investigates both self-focusing and self-phase-modulation (SPM) effects encountered by a strongly focused femtosecond pulse in a NPP crystal close to the SHG phase-matching resonance. Similarly, we compare our model with our experimental results obtained with a femtosecond optical parametric oscillator (OPO) tuned near the noncritical phase-matching (NCPM) wavelength of 1165 nm.

2. TEMPORAL NONLINEAR PROPAGATION

Following Eckhardt and Reintjes, the equations of motion for SHG for a type I interaction can be derived.[18] Here we use a retarded time frame moving with the fundamental field, thus eliminating the effects of temporal walk-off in the equation of motion for the fundamental field envelope:

$$\frac{\partial E_1}{\partial z} + \frac{ik_1''}{2}\frac{\partial^2 E_1}{\partial t^2} = i\Gamma E_2 E_1^* \exp(-i\Delta k z)$$

$$\frac{\partial E_2}{\partial z} - (k_1' + k_2')\frac{\partial E_2}{\partial t} + \frac{ik_2''}{2}\frac{\partial^2 E_2}{\partial t^2} = i\Gamma E_1 E_1 \exp(i\Delta k z). \quad (2)$$

Note that to derive Eqs. (2) we assumed the slowly varying envelope approximation on the envelope of the field $E_{1,2}$ as well as a Taylor expansion in the dispersion of the refractive index, so the propagation constant k is expanded to second order in frequency. In addition, to derive the driving terms on the right-hand sides of Eqs. (2) we have assumed that the bandwidth associated with the pulse is smaller than the optical frequency, making the coupling coefficient Γ a constant with respect to frequency. In the case of NPP, $\Gamma = 140\ \text{cm}^{-1}$ for 1 GW/cm^2. This indicates that for propagation of less than 100 μm a fundamental field of 1 GW/cm^2 could result in almost complete depletion without the presence of temporal walk-off. The dispersion of the nonlinear susceptibility is neglected. Such an approach was recently implemented to describe the effects of cascaded nonlinearities in ultrafast OPA's.[19] Figure 1 shows the spectral dependence of the material's dispersion parameters derived from Sellmeier's equations[15]: walk-off length and dispersion length for a 100-fs pulse. Note that the most relevant length for realistic crystal thicknesses is the so called walk-off length. We include group-velocity dispersion to take into account the spectral envelope of the field.[20] In the inset of Fig. 1 we show the dispersion length for the second-harmonic field at those wavelengths at which it may become comparable with a NPP crystal length, in particular, at the NCPM wavelength of 1165 nm.

Here we concentrate on spectral shape distortions. Our approach is driven from an experimental point of

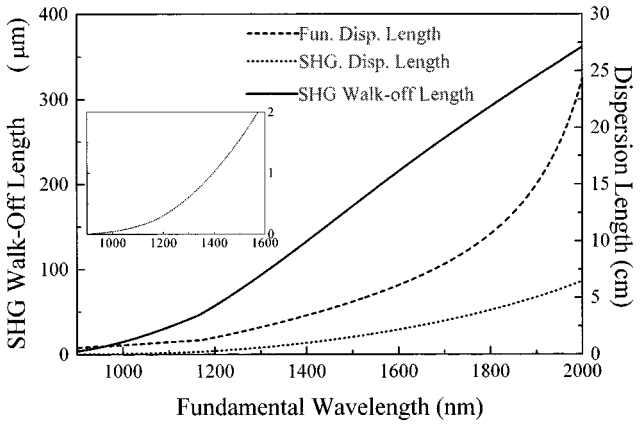

Fig. 1. Dispersion of the walk-off length and the group-velocity dispersion length, defined, respectively, as $L_w = \tau/|k_1' - k_2'|$ and $L_d^{1,2} = \tau^2/k_{1,2}''$. In our calculations we used a pulse width of 100 fs. Note that for lengths of several millimeters even picosecond pulses will endure strong walk-off effects.

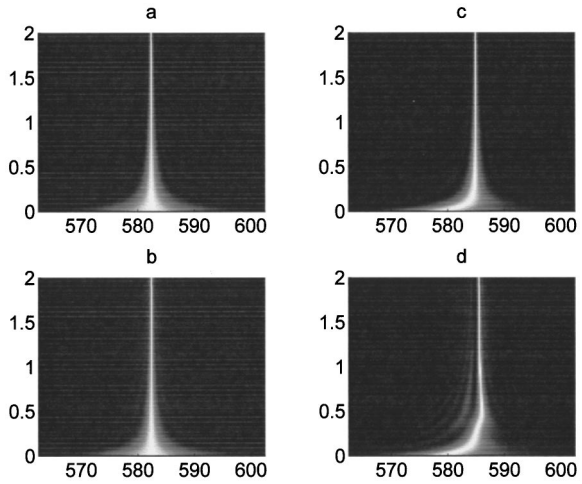

Fig. 2. Contours of the evolution of the SHG spectrum under the low-depletion approximation at phase matching corresponding to the NCPM wavelength of 1165 nm for a, 150 fs and 1 MW/cm^2 and b, 150 fs and 500 MW/cm^2. In both cases the abscissa is the fundamental wavelength in nanometers and the ordinate is the propagation distance in millimeters. The stronger effect is the narrowing of the second-harmonic spectrum compared with the input fundamental spectrum. c, d Show similar contours for the detuned case in which the fundamental peak wavelength is 1160 nm. In this case a spectral shift as well as an asymmetric spectrum with large sidebands results from the combined effects of the detuning and walk-off. The SHG spectra are all normalized to the same magnitude.

view; indeed, temporal SPM is one of the most useful techniques for observing cascaded second-order nonlinearities.[20] We now assume that no second harmonic is launched at the entrance of the nonlinear device and that the fundamental is not depleted by the SHG and thus remains unchanged while propagating in the nonlinear medium. The envelope is then only time dependent. If we now Fourier transform Eqs. (2), which describe the evolution of the second-harmonic field envelope, we obtain the following solution for the spectral power envelope of the SHG field:

$$|E_2{}^{\omega}| = \Gamma^2 F(\omega)^2 z^2 \sin c^2 \times \left([\Delta k - \omega(k_1' + k_2'') - \omega^2 k_2''] \frac{z}{2} \right), \quad (3)$$

where $F(\omega)$ is the Fourier spectrum of the square of the fundamental field envelope and ω refers to the Fourier component of the field modulated with a central optical frequency. $\Omega = \Omega_c + \omega$, where Ω is the optical angular frequency, Ω_c is the carrier frequency, and ω is the Fourier component that describes the shape of the pulse envelope. Note that in the case of a long pulse or equivalently of a narrow fundamental spectrum we find the usual SHG response function, where $\omega = 0$, dispersion can be neglected, or both. In the other interesting limit, in which the sinc function is narrower then the spectral

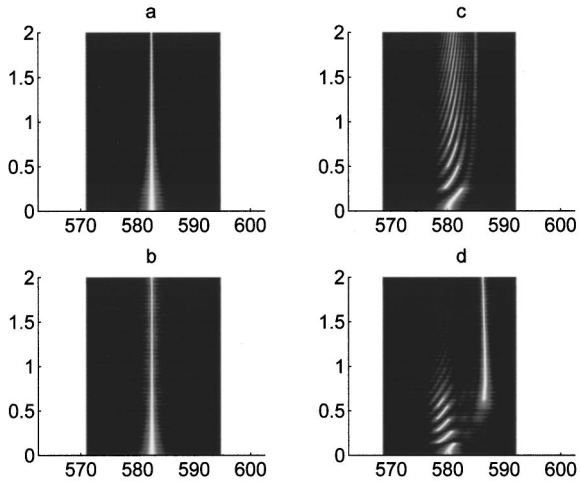

Fig. 3. Contours of the spectral evolution of the second-harmonic when Eqs. (2) are numerically integrated for 750 fs with an initial fundamental spectrum centered at a, b, 1165 nm and c, d, 1160 nm for weak and strong depletion conditions of c, d, 1-MW/cm^2 and b, d, 500-MW/cm^2 fundamental input intensities.

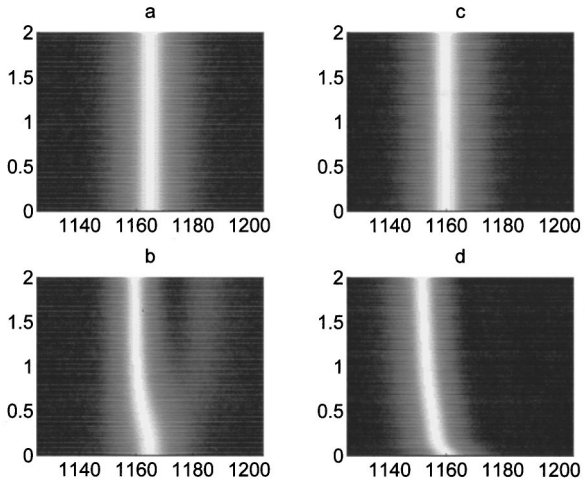

Fig. 4. Evolution of the fundamental spectrum at low powers: a, 1 MW/cm^2 at phase matching and b, 500 MW/cm^2 at 1165 nm. Similar highly modulated and shifted spectra are observed when the intensity is increased at c, d, 1160-nm input central wavelengths.

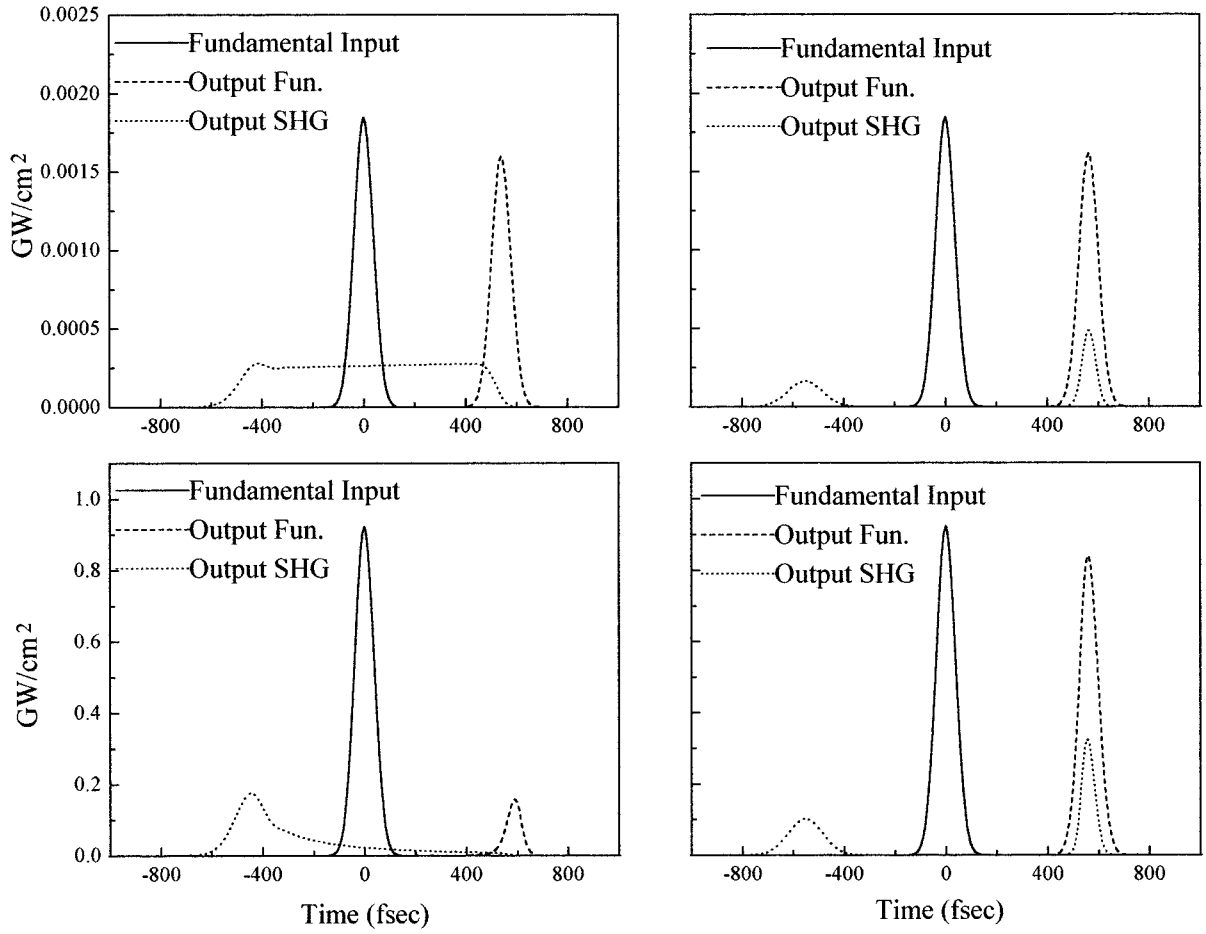

Fig. 5. Output temporal profiles for fundamental and second-harmonic intensities for the same conditions as for Figs. 2 and 4. In the second harmonic has been multiplied by a factor of 200 in a, by a factor of 10^4 in c, and by a factor of 100 in d.

bandwidth of $F(\omega)$, ultrafast pulses propagating in NPP, for example, the centroid of the SHG spectrum is shifted toward $\omega_0 \approx \Delta k/(k_1' + k_2')$, assuming that the group-velocity dispersion is negligible. The spectrum also has taken the shape of the sinc^2 function, narrowing the SHG spectrum and thus resulting in a long squarelike pulse in time. Note that such a spectral shift can also be obtained with higher-order dispersion.[21] These conclusions are reminiscent of early results for ultrashort pulses as well as of more recent research, which deals with such effects in greater detail.[22–24] Figure 2 shows the evolution of the SHG spectrum as the pulse propagates in the NPP crystal according to Eqs. (2). We integrated Eqs. (2) numerically for a series of input conditions. Both fundamental and second-harmonic propagation losses were taken into account.[15] In general, good agreement between our numerically integrated Eqs. (2) was found with Eq. (3) derived for low depletion. Note that at the maximum of the phase-matching resonance the centroid of the SHG spectrum remains locked in a position corresponding to the maximum of the fundamental field spectrum, whereas off-phase matching of the sinc^2 function can be approximated by a $\sin^2$ function evolving into a narrower SHG spectrum and shifting its centroid toward $\omega_0 \approx \Delta k/(k_1' + k_2')$. For comparison, Fig. 3 shows the evolution of the SHG spectrum when Eqs. (2) are integrated for longer pulses, 750 fs long, for two phase-matching cases. Note that the general shape of the evolution remains unchanged. The SHG spectrum narrows at both low and high powers, and off-phase matching forms a strong sideband at a wavelength shifted from the central spectral position of the fundamental input. The shift is considerably smaller because we are dealing with a case that more closely resembles the usual cw case in which, for instance, $\omega \approx 0$ in Eq. (3). The temporal evolution results in the expected SHG long pulse's being formed in the presence of large walk-off. Note that the intensities used are relatively low, 1 and 500 MW/cm^2.

Inverse Fourier transforming the complex spectral amplitude of the second-harmonic field in the limit of large walk-off and thus assuming a narrow spectrum for the SHG field results in the following equation of motion:

$$\frac{\partial E_1{}^{\omega}}{\partial z} = i\,\frac{k_1''}{2}\,\omega^2 E_1{}^{\omega} - i\Gamma^2 F(\omega_0) z (E_1{}^{\omega})^*. \qquad (4)$$

Note that the first term on the right-hand side of Eq. (4) corresponds to the standard linear chirp produced by the

group-velocity dispersion and the second term produces an intensity-dependent power broadening, the cascading term. The effects of walk-off are felt by the $F(\omega_0)$ term. Only the Fourier component at $\omega_0 \approx \Delta k/(k_1' + k_2')$ contributes to the power broadening, whereas in the small-walk-off case the whole spectrum would contribute. No dramatic redistribution of the power spectrum can be expected under the low-depletion approximation. The fundamental field will thus retain its shape, as expected in the negligible nonlinearity case.[25] Equivalently, SPM measurements of the fundamental spectral broadening will typically not be sensitive enough to permit such small temporal phase changes to be measured. An approximate expression can be derived for the phase chirp induced by the group-velocity dispersion and the cascaded second-order nonlinearity for each fundamental Fourier component of the pulse:

$$\Delta\Phi_1{}^{\omega} = \frac{k_1''}{2}\,\omega^2 z - \Gamma^2 F(\omega_0)\,\frac{z^2}{2}. \tag{5}$$

Note that for large spectral shifts of the second-harmonic spectrum, or equivalently for large detunings and group velocities, the effects of cascaded nonlinearities will be strongly reduced by the monotonic decay of $F(\omega)$. Equivalently, in the time domain the overlap between the fundamental and the second-harmonic pulses is strongly reduced, limiting the cascading efficiency. For small propagation distances, long pulses, or both, the first term of Eq. (5) can be neglected, as indicated by Fig. 1.

We show in Fig. 4 the evolution of the fundamental in the case of NPP for both the low-depletion case and a strong fundamental depletion, for 150-fs long pulses with conditions similar to those used for Fig. 2. Note that the fundamental spectral shape remains mostly unchanged at low powers and that only large intensities will affect its spectral distribution at and off NCPM. Such spectral redistributions and distortions are evidence of cascaded effects with a strong interplay among the linear propagation, walk-off, and the nonlinearity. However, the temporal distributions of the fundamental and the second harmonic are strongly affected, rendering their further use difficult in an interferometric device such as an all-optical switch that uses both fields; see Fig. 5. This situation is reminiscent of the pulse breakup problem in third-order nonlinear switching, which could be solved by the implementation of switches with longer pulses or temporal solitons. In our case the latter solution seems unlikely, and, although longer pulses may be appropriate to reduce such problems, they imply higher energies per pulse. Large walk-off effects will dramatically increase the energy level required for switching, as we show in Section 3.

3. SPATIAL NONLINEAR PROPAGATION

From Fig. 1, an immediate solution to the temporal walk-off issues evoked in Section 2 would be to use longer pulses at wavelengths at which the temporal walk-off length is large. For example, at wavelengths near 1550 nm, the third telecommunication window, Fig. 1 seems to indicate that temporal walk-off and dispersion would be resolved. Unfortunately, as is well known, at wavelengths away from NCPM (1165 nm) short spatial walk-off lengths are present in NPP. Figure 6 shows the walk-off length, defined as the length for which a beam is displaced by a full width. We used 100 μm as the initial beam width (half-width at $1/e^2$). To model the nonlinear propagation in the cw case we take the same numerical approach used for the recent discovery of multidimensional solitary waves in type II SHG in KTP.[9] The equations of motion for the fundamental and the SHG fields for type I phase matching are as follows:

$$\frac{\partial E_1}{\partial z} - \frac{i}{2k_1}\left(\frac{\partial^2 E_1}{\partial x^2} + \frac{\partial^2 E_1}{\partial y^2}\right) = i\Gamma E_2 E_1{}^{*} \exp(-i\Delta k z),$$

$$\frac{\partial E_2}{\partial z} - \rho_{2\omega}\frac{\partial E_2}{\partial x} - \frac{i}{2k_2}\left(\frac{\partial^2 E_1}{\partial x^2} + \frac{\partial^2 E_1}{\partial y^2}\right) = i\Gamma E_1 E_1 \exp(i\Delta k z), \tag{6}$$

where we have assumed the paraxial approximation and cw operation. $\rho_{2\omega}$ is the tangent of the walk-off angle. We have assumed a close-to-phase-matching geometry at 1064 nm, which is obtained in an $oo \rightarrow e$ geometry. For fundamental wavelengths longer than the NCPM wavelength the walk-off will be seen by the fundamental beam by an $ee \rightarrow o$ interaction.[15] Note that at the fundamental of Nd:YAG the walk-off angle is approximately 14°, which corresponds to a walk-off length of 800 μm with $L_w = 2w_0/\tan(\rho_{2\omega})$ for a beam waist of 100 μm (Fig. 6). For an efficient cascaded effect a good spatial overlap is necessary between the fundamental and the second-harmonic beams. Because of the lateral displacement induced by walk-off, the effective interaction length at which a nonlinear phase shift can be accumulated is considerably reduced, even with as large a nonlinearity as encountered in NPP. In as much as only large-diameter beams can be used, in bulk materials the energy per pulse necessary for switching is increased. On the other hand, in strongly waveguided geometries the modes of propagation are hybrid in nature, rendering modeling difficult but with only the temporal walk-off remaining a relevant issue. In what follows we show our numerical and experimental results for a coherent switch in which type I phase matching was used. In terms of switching energies our results are an order of magnitude better than those obtained with KTP.[10] However, an improvement of 3 orders of magnitude would be expected from the material's figure of merit alone.

Switching, or transistor action, can be seen in a SHG process in which a weak coherent seed wave is input to a crystal with a strong fundamental wave. The effect of the seed wave is to alter the phase-matching conditions. Hence the output fundamental can be changed from substantial depletion to almost no depletion by modulation of either the phase or the amplitude of the weak seed. Such behavior was recently theoretically predicted and experimentally demonstrated in KTP.[7,8,10] Following the same approach used in our earlier KTP experiment,[10] we generated 30-ps long (FWHM) pulses from a passively mode-locked and Q-switched Nd:YAG laser. Single pulses were extracted, extracavity, from the train of pulses with an electro-optic pulse selector. We then collimated the

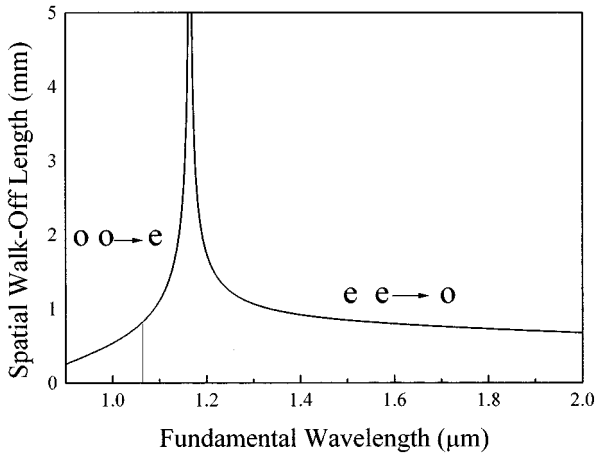

Fig. 6. Walk-off length, $L_w = 2\omega_0/\tan(\rho_{2\omega})$, where $\omega_0 = 100$ μm and $\rho_{2\omega}$ is calculated from the refractive-index dispersion.[15] At 1.064 μm the walk-off length is ~800 μm.

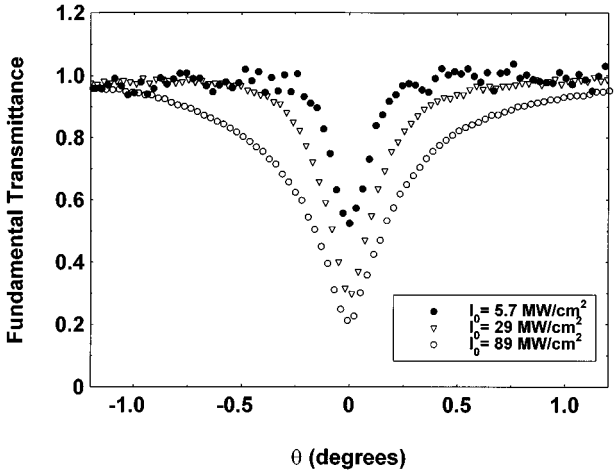

Fig. 7. Experimentally measured depletion as a function of the phase-matching angle θ. Note that beyond 5 MW/cm^2 little improvement is obtained because of the combined effects of walk-off and linear absorption at the second harmonic. Nonlinear absorption at 532 nm at the phase-matching angle for a 1.064-μm fundamental was measured to be less than 1 cm/GW.

fundamental beam and sent it through a 3-cm-long KDP crystal to generate a coherent second-harmonic beam to a level of a few microjoules, making sure that no strong depletion was present on the fundamental beam. We verified that both beams were Gaussian in shape and propagation, with an ellipticity of less than 10%. We controlled the relative phase between the fundamental and the second harmonic with a variable-pressure nitrogen cell, taking advantage of the small pressure dependence of the dispersion between both wavelengths. Both beams were collinearly focused onto the entrance face of the 2-mm long NPP sample to a spot size w_0 that varied from 20 to 350 μm (half-width at $1/e^2$). Before measuring switching action we studied the SHG properties of the NPP crystal with those pulses. The depletion curves, shown in Fig. 7, were in good agreement with expected calculations; however, increasing the intensity beyond 5 MW/cm^2 did not increase the SHG efficiency. We believe that the latter effect is due to the combined effects of walk-off and linear loss at 532 nm. Nonlinear loss measurements with Z scan showed a two-photon absorption coefficient at 532 nm of less than 1 cm/GW at the phase-matching angle for SHG of 1064-nm radiation. With the same orientation no multiphoton absorption was measurable for the fundamental at the intensities used in our experiments, up to 2 GW/cm^2. The transmission of the fundamental beam as a function of the relative phase or, equivalently, of the pressure in the nitrogen cell was monitored with a calibrated detector and a silicon camera, which were both placed after the NPP sample. Fig-

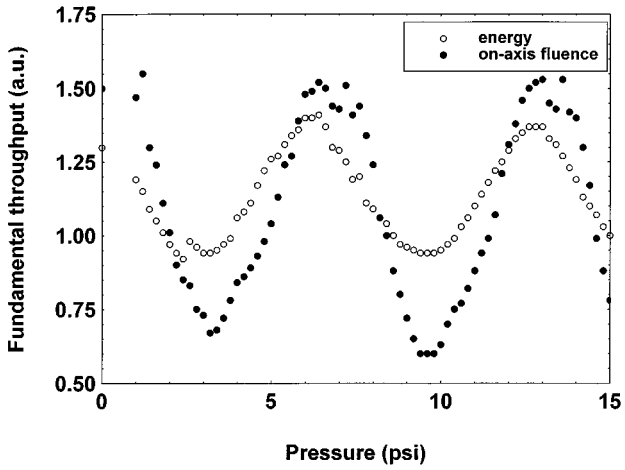

Fig. 8. Experimentally obtained modulation of the transmission with an input fundamental intensity of 1 GW/cm^2. The pressure was calibrated so that 6 psi corresponds to a relative phase difference of 2π between fundamental and SHG.

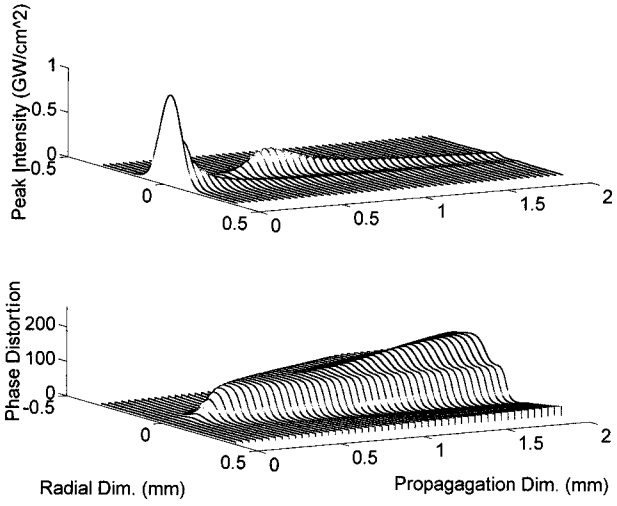

Fig. 9. Spatial evolution of the amplitude and the phase of the fundamental field as it propagates through a 2-mm-long NPP crystal for an input beam waist of 100 μm, for a 1-GW/cm^2 input intensity. In this geometry the largest effect is due to spatial walk-off; beam diffraction can be neglected. The fundamental wavelength is 1.064 μm.

ure 8 shows such a modulation fraction as a function of the gas cell pressure, where 6 psi (1 psi = ~52 Torr) corresponds to 2π from our previous experimental calibration.[10] We show measurements of modulation of the total transmitted fundamental energy as well as of the on-axis fluence of the fundamental. KTP provided us with a slightly better contrast ratio; however, such modulation was expected at lower peak intensities for NPP. Indeed, the material figure of merit for NPP is almost 3 orders of magnitude higher than that of KTP. Only a 1-order-of-magnitude improvement was experimentally measured. Figure 8 was obtained for an input intensity of 1 GW/cm^2 (an intensity of 20 GW/cm^2 was used for KTP with similar results) and an 8% or 80-MW/cm^2 SHG seeded at the entrance face of the NPP crystal.[10] Even though the SHG efficiency scales properly with the figure of merit and large depletions are obtained for input intensities as low as 5 MW/cm^2, because the phase distortion induced by cascaded effects is length dependent it is more sensitive to walk-off effects. Whereas in standard SHG walk-off reduces the efficiency but does not prevent the generation, in the case of cascading backconversation is required, and a portion of the field is lost: The overlap between the fundamental and the second harmonic is reduced. An inspection of the equations of motion, Eqs. (2) and (6), indicates that the presence of the second-harmonic field plays an additive role in the second-harmonic equation of motion and a multiplicative role in the downconversion equation of motion. The latter effect raises the switching intensity by as much as a factor of 50 from what was originally expected from the material figure of merit. We believe that most of the reduced switching efficiency is thus due to the presence of large spatial walk-off effects at 1.064 μm.

To show the effects of spatial walk-off on such a switching experiment, we show the calculated spatial evolution of the fundamental field in the presence of walk-off. We do this by numerically integrating Eqs. (6), as a function of propagation distance, with a fundamental input of 1 GW/cm^2 and no second harmonic present at the entrance face. The results are shown in Fig. 9. As can be seen, not only is the amplitude of the fundamental redistributed during propagation, rendering switching incomplete, but the fundamental phase front is aberrated, making a coherent switch less efficient. For comparison the time-averaged spatial profiles measured at the output of the NPP crystal are shown in Fig. 10. The amplitude distortion induced by the strong spatial walk-off is clear. As a

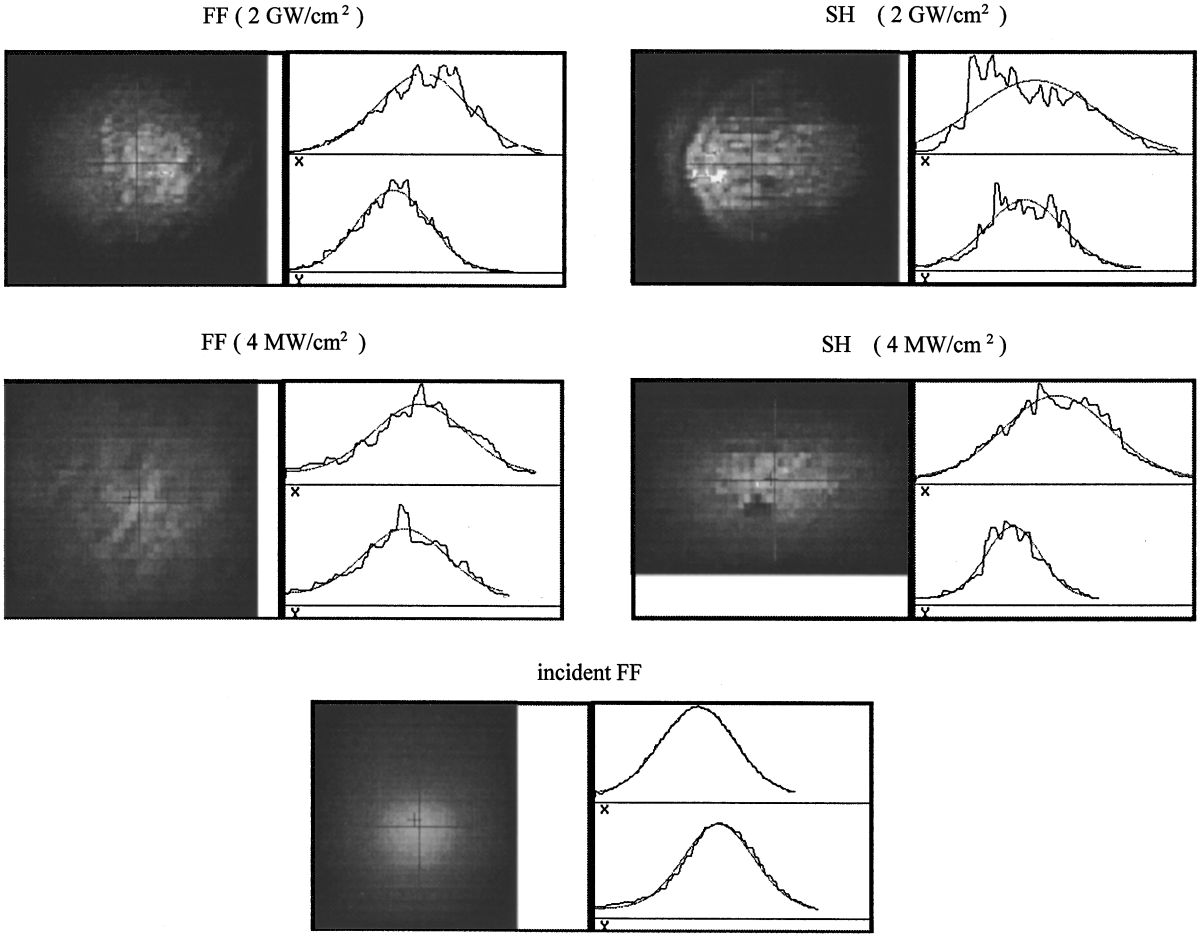

Fig. 10. Spatial profiles of the fundamental (FF) and the second harmonic (SH) at the output of a NPP crystal oriented for SHG phase matching. For comparison we show the beam profile at the same location without the crystal's being present.

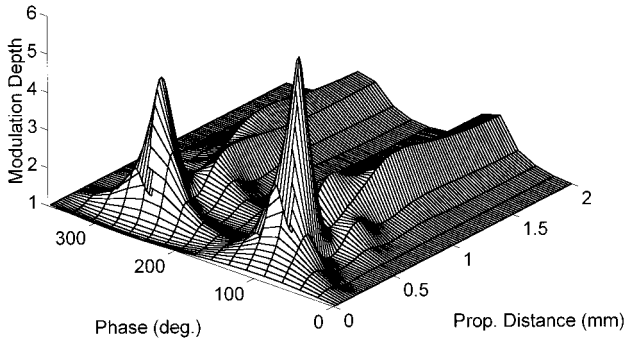

Fig. 11. Evolution of the transmission modulation ratio[10] as a function of the propagation length in NPP for an input intensity of 1 GW/cm^2 at 1.064 μm and a phase mismatch $\Delta kL = \pi/3$. Note that for this intensity the best length corresponds to a short 200-mm-thick crystal, for which walk-off effects may not be important.

consequence we can estimate the modulation ratio as a function of propagation, which compares reasonably well with our experimental measurements, as shown in Fig. 11. Note that at this input intensity an optimized modulation would have been found for a shorter crystal, for which walk-off effects may be negligible. The maximum modulation is in reasonable agreement with our experimental data reported in Fig. 8. The doubled periodicity was not reproduced experimentally because, we believe, our model is cw and a numerical integration in time needs to be performed for each phase condition as a result of the strong fundamental beam aberration. Such doubled periodicity is another evidence of the presence of large walk-off in NPP, which was not present in similar calculations performed for KTP. Such calculations were in excellent agreement with the KTP switching experiments.[10]

4. SPATIOTEMPORAL NONLINEAR PROPAGATION

Recently there has been renewed interest in ultrafast propagation in nonlinear materials[26,27] because of the appearance of tunable ultrafast laser sources, which can be amplified beyond terawatts.[29–31] Numerical models have shown the ability to predict adequately the mode locking of Ti:Al_2O_3 lasers that is due to self-focusing in the laser crystal.[31] Such interest is also driven from a fundamental point of view; for instance, strong coupling of a Maxwell–Bloch system can lead to new forms of electromagnetic radiation,[32] and because of the large bandwidths obtained standard approximations such as the slowly varying envelope approximation can be violated.[33] Here we employ such approaches to predict accurately and understand the propagation of an ultrafast pulse focused into a highly nonlinear and dispersive material such as NPP. We specifically want to reproduce the temporal modulation that is due to SPM measured near the NCPM wavelength and the measured SHG efficiency. We measured the SPM spectral broadening and modulation by focusing the output of a commercial OPO, OPAL from Spectra-Physics, Inc., onto the 2-mm-long crystal. The OPO was synchronously pumped by a Kerr-lens mode-locked Ti:Al_2O_3 laser emitting 150-fs pulses at an 82-MHz repetition rate. The mirrors and the output coupler of the OPO were chosen so that it was tunable on the signal side from 1100 to 1300 nm and also produced 150-fs-long pulses (FWHM), which our time–bandwidth product measurements showed to be chirp free. To observe the spectral broadening that is due to temporal SPM we focused the output of the OPO into the same 2-mm-thick NPP and optimized the focusing and the crystal orientation for maximum SHG efficiency. The focused beam waist was 8 μm. The output spectrum was recorded with a spectrometer at low and high powers. To model our experimental results accurately with such a strongly focused beam we developed a code with one transverse spatial and one temporal dimension. Such an approach was recently used to design and predict the behavior of a mode-locked laser.[31] In essence this approach embodies the procedures described in the Sections 2 and 3. Because the group-velocity dispersion term is positive, no

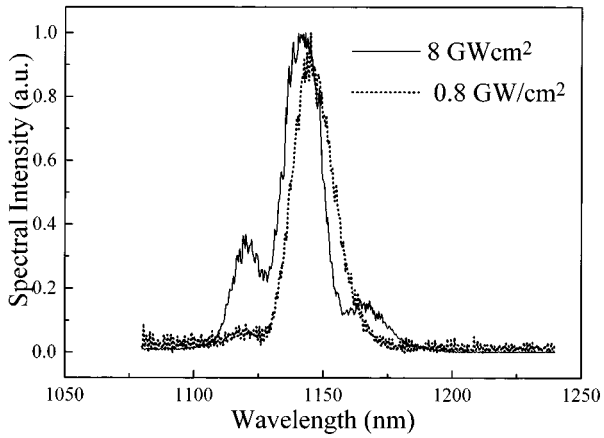

Fig. 12. Spectral broadening at the NCPM wavelength for 8- and 0.8-GW/cm^2 peak intensities at the focus of an 8-μm waist in NPP. We experimentally measured the NCPM to be located at 1150 nm rather than the 1165 nm obtained from the Sellmeier equations.

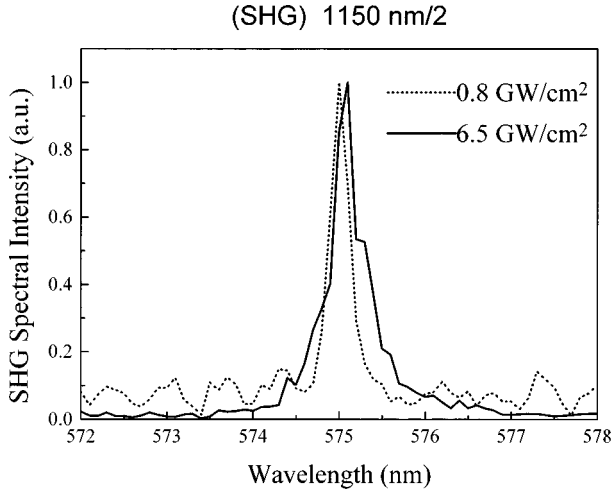

Fig. 13. Spectrum of the second-harmonic beam at the NCPM wavelength for intensities similar to those shown in Fig. 12.

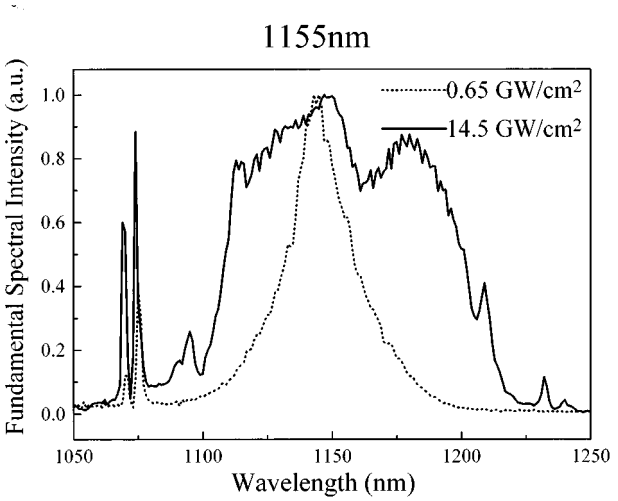

Fig. 14. SPM spectral broadening away from NCPM. The narrow lines observed on the blue side of the spectra are spectral ghosts of the second harmonic.

collapse is expected, as was recently reported.[34] Indeed, the spatiotemporal rays see not a parabolic potential but a saddle-shaped one,[35] as can be found from the governing equations that model our experiments:

$$\frac{\partial E_1}{\partial z} + \frac{ik_1''}{2}\frac{\partial^2 E_1}{\partial t^2} - \frac{i}{2k_1}\frac{\partial^2 E_1}{\partial x^2} = i\Gamma E_2 E_1^* \exp(-i\Delta k z),$$

$$\frac{\partial E_2}{\partial z} - (k_1' + k_2')\frac{\partial E_2}{\partial t} + \frac{ik_2''}{2}\frac{\partial^2 E_2}{\partial t^2} - \frac{i}{2k_2}\frac{\partial^2 E_2}{\partial x^2} = i\Gamma E_1 E_1 \exp(i\Delta k z). \quad (7)$$

Because we are operating near the NCPM wavelength, spatial walk-off was neglected. In addition, all our observations show cylindrically symmetric behavior. We can thus model the propagation by two-dimensional fast Fourier transforms with one dimension in time and the other in space while maintaining the correct dependence of the diffracted field in three dimensions and maintaining a reasonable and accessible computing time. It is clear that the inclusion of a second spatial dimension is necessary for a full analysis of the propagation in time and space. However, the physical mechanisms accessible with such a more accurate approach are beyond the scope of this study. We assume that we are operating in a regime where the slowly varying envelope approximation is valid and no strong spatiotemporal focusing is present.[33]

As expected from the temporal propagation discussion, we did not observe large spectral broadening at the NCPM wavelength. However, at large peak intensities sidelobes where observed, as shown in Fig. 12, which can be attributed to the temporal walk-off between fundamental and harmonic waves. An initial shift of the fundamental peak wavelength can also be observed that is due to pump depletion and strong temporal walk-off. Similarly, the second-harmonic spectra were always narrow compared with the fundamental input spectra, as expected and shown experimentally in Fig. 13. On the other hand, away from NCPM, large intensity-dependent spectral broadening and modulation of the fundamental beam are observed. An example is presented in Fig. 14. Far away from the NCPM wavelength, 1200 nm for example, such broadening is not seen. Although it can be reproduced qualitatively with the temporal model discussed in Section 2, the intensity dependence is poorly reproduced by such a simple model. This result can be expected, as we focused the output of the OPO at 8 μm, which corresponds to a 350-μm depth of focus, almost an order of magnitude smaller than the crystal length. From our spatial modeling [Eqs. (6)] we could predict strong spatial effects at large intensities in such a strong focusing case. The model represented by Eqs. (7) was thus implemented. The nonlinearly coupled equations were integrated in time and space in the Fourier domain, which made full use of two-dimensional fast Fourier transforms, whereas the nonlinear coupling was integrated with a second-order Runge–Kutta routine. This procedure resembles the approach taken to model the propagation of solitary waves in KTP, which resulted in

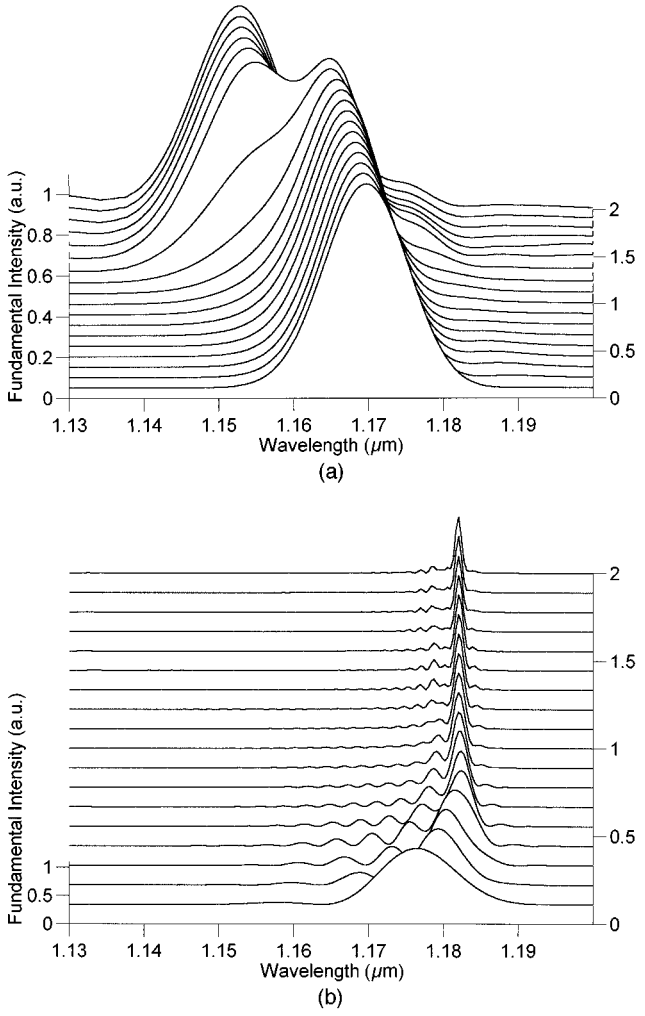

Fig. 15. Simulated evolution of (a) the fundamental and (b) the second-harmonic spectra for an intensity at focus of 10 GW/cm^2. The spectra have all been normalized to unity; large broadening owing to cascaded SPM and shifts owing to walk-off are observed.

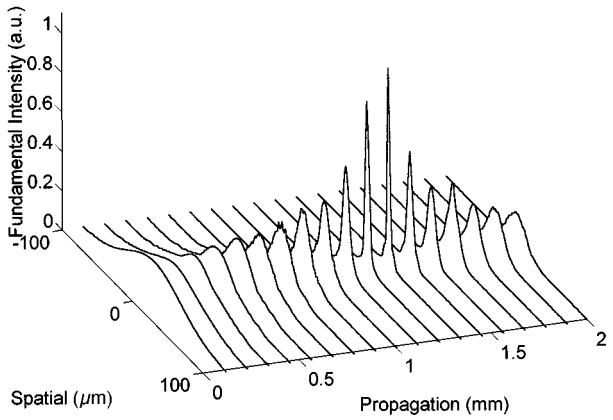

Fig. 16. Simulated evolution of the fundamental spatial profile with the same conditions used for Fig. 15. The beam was initially focused 1 mm behind the sample. Because of cascaded self-focusing the focused spot is now inside the NPP sample.

good agreement between experiments and model.[9] Here this approach, in which in addition to the previously described beam-propagation method the appropriate focusing was assumed for the input fundamental, also shows good agreement. We included linear absorption coefficients at both the fundamental, 2.5 cm^{-1}, and the second harmonic, 8.5 cm^{-1}.

Because of the strong linear absorption the best SHG efficiency was obtained when the beam was focused upon a plane located slightly behind the sample. This optimization is easily understood: If the SHG is generated close to the entrance face it will see a large absorption, whereas when the fundamental is weakly focused it can continue to generate the second harmonic without losing its strength too quickly, rendering the effective length for which a nonlinear phase can be accumulated comparable with almost the full crystal length. In a sense we have a tapered waveguide geometry. However, a significant difference exists in that the waveguide geometry is intensity dependent because of the combined effects of self-focusing and self-phase modulation. We show such evolution in Figs. 15 and 16. Our modeling predicts that at peak intensities of 8–10 GW/cm^2 a SHG efficiency of 20% can be reached with femtosecond pulses in a 2-mm-long NPP crystal. Higher efficiencies could be obtained with a shorter crystal with which the SHG would not suffer from the strong linear absorption and temporal broadening that are due to walk-off.

5. CONCLUSION

In conclusion, we have shown that the nonlinear propagation of collimated and strongly focused beams in NPP close to SHG phase matching can be adequately understood with our nonlinear propagation modeling even in the case of ultrashort fundamental pulses when walk-off in time, in space, or in both is properly taken into account. Because of the large spatial walk-off encountered away from the NCPM wavelength, leading to effective lengths of the order of a few tens to hundreds of micrometers, bulk NPP does not result in the expected enhancement or lowering of the energy required for a coherent switch to operate. Similarly, when NPP is operated near NCPM, long pulses are still required if one is to avoid the detrimental effects of temporal walk-off. It is clear that the nonlinearity is effectively large only when short samples can be used, at the expense of higher pulse energies required for switching. In the case of harmonic or parametric generation or amplification such an implication may not be so detrimental as it is for cascaded all-optical-switching applications. Materials with QPM structures are probably the answer to such problems. Indeed, no spatial walk-off will be present in QPM structures, and picosecond pulses with effective lengths of several millimeters can be used without temporal walk-off effects at telecommunication wavelengths. Linear losses at those wavelengths remain to be reduced as well. Fabricating such an ideal material is still a challenging project for materials scientists. With the recent advances in inorganic bulk and waveguide QPM devices the advent of an organic QPM structure with nonlinearities approaching 100 pm/V seems to be within reach.

ACKNOWLEDGMENTS

The authors have the pleasure to acknowledge interesting discussions at the Center for Research and Education in Optics and Lasers with G. I. Stegeman and G. Assanto as well as with J. Kafka of Spectra-Physics, Inc. W. E. Torruellas is indebted to Robert Wolf of Spectra-Physics for the opportunity to perform the OPO measurements.

REFERENCES

1. G. I. Stegeman and W. E. Torruellas, "Nonlinear materials for information processing and communications," Philos. Trans. R. Soc. London (March 1995).
2. M. Sheik-Bahae, D. J. Hagan, and E. W. VanStryland, Phys. Rev. Lett. **65,** 96 (1990).
3. G. I. Stegeman, R. Schiek, L. Torner, W. Torruellas, Y. Baek, D. Baboiu, Z. Wang, E. VanStryland, D. Hagan, and G. Assanto, "Cascading: a promising approach to nonlinear Optical Phenomena Revisited," in *Novel Optical Materials and Applications*, I. C. Khoo and F. Simoni, eds. (Wiley Interscience, New York, 1995).
4. L. A. Ostrovsky, Pis'ma Zh. Eksp. Teor. Fiz. **5,** 331 (1967).
5. M. Fejer, Phys. Today **40**(5), 25 (1994).
6. Y. Baek, R. Schiek, and G. I. Stegeman, Opt. Lett. **20,** 2168 (1995); R. Schiek, Y. Baek, G. Krijnen, G. I. Stegeman, I. Baumann, and W. Sohler, "All-optical switching in lithium niobate directional couplers with cascaded nonlinearity," Opt. Lett. **21,** 940 (1996).
7. G. Assanto, G. I. Stegeman, M. Sheik-Bahae, and E. VanStryland, IEEE J. Quantum Electron. **31,** 673 (1995).
8. P. St. J. Russell, Electron. Lett. **29,** 1228 (1993).
9. W. E. Torruellas, Z. Wang, D. J. Hagan, E. W. VanStryland, G. I. Stegeman, L. Torner, and C. R. Menyuk, Phys. Rev. Lett. **74,** 5036 (1995).
10. D. J. Hagan, Z. Wang, G. I. Stegeman, E. W. VanStryland, M. Sheik-Bahae, and G. Assanto, Opt. Lett. **19,** 1305 (1995).
11. L. Lefort and A. Barthelemy, Electron. Lett. **31,** 910 (1995).
12. G. Assanto, Z. Wang, D. J. Hagan, and E. W. VanStryland, Appl. Phys. Lett. **67,** 2120 (1995).
13. Z. Wang, "Nonlinear phase shifts in second-order optical nonlinearities: theory and applications," Ph.D. dissertation (University of Central Florida, Orlando, Fla., 1996).
14. W. E. Torruellas, D. Y. Kim, M. Jaegger, G. Krijnen, R. Schiek, G. I. Stegeman, P. Vidakovic, and J. Zyss, in *Polymers for Second-Order Nonlinear Optics*, G. A. Linsay and

K. D. Singer, eds. ACS Symposium Ser. **601**, 509–521 (1995).
15. I. Ledoux, C. Lepers, A. Perigaud, J. Badan, and J. Zyss, Opt. Commun. **80,** 149 (1990).
16. I. Ledoux, J. Badan, J. Zyss, A. Migus, D. Hulin, J. Etcheparе, G. Grillon, and A. Antonetti, J. Opt. Soc. Am. B **4,** 987 (1987).
17. D. Josse, S. X. Dou, J. Zyss, P. Andreazza, and A. Perigaud, Appl. Phys. Lett. **61,** 121 (1992).
18. R. Eckardt and R. Reintjes, IEEE J. Quantum Electron. **20,** 1178 (1984).
19. F. Hache, A. Zeboulon, G. Gallot, and G. M. Gale, Opt. Lett. **20,** 1556 (1995).
20. M. L. Sundheimer, Ch. Bosshard, E. W. VanStryland, G. I. Stegeman, and J. D. Bierlein, Opt. Lett. **18,** 1398 (1993).
21. K. Naganuma and K. Mogi, Opt. Lett. **16,** 728 (1991).
22. J. Comly and E. Garmire, Appl. Phys. Lett. **12,** 7 (1968).
23. P. P. Ho, D. Ji,Q. Z. Wang, and R. R. Alfano, J. Opt. Soc. Am. B **7,** 276 (1990).
24. E. Sidick, A. Knoesen, and A. Dienes, J. Opt. Soc. Am. B **12,** 1704 (1995).
25. G. P. Agrawal, *Nonlinear Fiber Optics* (Academic, London, UK, 1989).
26. Y. Silberberg, Opt. Lett. **15,** 1282 (1990).
27. N. Akhmediev and J. M. Soto-Crespo, Phys. Rev. A **47,** 1358 (1993).
28. G. G. Luther, J. V. Moloney, A. C. Newell, and E. M. Wright, Opt. Lett. **19,** 862 (1994).
29. E. Esarey, S. Sprangle, M. Piloff, and J. Krall, J. Opt. Soc. Am. B **12,** 1695 (1995).
30. J. Paye and A. Migus, J. Opt. Soc. Am. B **12,** 1480 (1995).
31. I. P. Christov, V. D. Stoev, M. M. Murname, and H. C. Capteyn, Opt. Lett. **20,** 2111 (1995).
32. A. E. Kaplan and P. L. Shkolnikov, Phys. Rev. Lett. **75,** 2316 (1995).
33. J. E. Rothenberg, Opt. Lett. **17,** 1340 (1992).
34. S. I. Liu, W. Z. Wang, and J. Z. Xu, Appl. Phys. Lett. **67,** 2774 (1995).
35. A. T. Ryan and G. P. Agrawal, J. Opt. Soc. Am. B **12,** 2382 (1995).